

# Achieving Frequency Reuse 1 in WiMAX Networks with Beamforming

Masood Maqbool, Marceau Coupechoux, Philippe Godlewski, Véronique Capdevielle

► **To cite this version:**

Masood Maqbool, Marceau Coupechoux, Philippe Godlewski, Véronique Capdevielle. Achieving Frequency Reuse 1 in WiMAX Networks with Beamforming. WiMAX, New Developments, In-Tech, pp.1-14, 2009. hal-01547160

**HAL Id: hal-01547160**

**<https://hal-imt.archives-ouvertes.fr/hal-01547160>**

Submitted on 26 Jun 2017

**HAL** is a multi-disciplinary open access archive for the deposit and dissemination of scientific research documents, whether they are published or not. The documents may come from teaching and research institutions in France or abroad, or from public or private research centers.

L'archive ouverte pluridisciplinaire **HAL**, est destinée au dépôt et à la diffusion de documents scientifiques de niveau recherche, publiés ou non, émanant des établissements d'enseignement et de recherche français ou étrangers, des laboratoires publics ou privés.

# Achieving Frequency Reuse 1 in WiMAX Networks with Beamforming

Masood Maqbool, Marceau Coupechoux, Philippe Godlewski  
*TELECOM ParisTech & CNRS LTCI, Paris  
France*

Véronique Capdevielle  
*Alcatel-Lucent Bell Labs, Paris  
France*

In this chapter, we examine the performance of adaptive beamforming in connection with three different subcarrier permutation schemes (PUSC, FUSC and AMC) in WiMAX cellular network with frequency reuse 1. Performance is evaluated in terms of radio quality parameters and system throughput. We show that organization of pilot subcarriers in PUSC Major groups has a pronounced effect on system performance while considering adaptive beamforming. Adaptive beamforming per PUSC group offers full resource utilization without need of coordination among base stations. Though FUSC is also a type of distributed subcarrier permutation, its performance in terms of outage probability is somewhat less than that of PUSC. We also show that because of lack of diversity, adjacent subcarrier permutation AMC has the least performance as far as outage probability is concerned. Results in this chapter are based on Monte Carlo simulations performed in downlink.

## 1. Introduction

Network bandwidth is a precious resource in wireless systems. As a consequence, reuse 1 is always cherished by wireless network operators. The advantage of reuse 1, availability of more bandwidth per cell, is jeopardized by increased interference because of extensive reutilization of spectrum. However, the emergence of new technologies like WiMAX, characterized by improved features such as advance antenna system (AAS), promises to overcome such problems.

Mobile WiMAX, a broadband wireless access (BWA) technology, is based on IEEE standard 802.16-2005. Orthogonal frequency division multiple access (OFDMA) is a distinctive characteristic of physical layer of 802.16e based systems. The underlying technology for OFDMA based systems is orthogonal frequency division multiplexing (OFDM).

In OFDM, available spectrum is split into a number of parallel orthogonal narrowband subcarriers. These subcarriers are grouped together to form subchannels. The distribution of subcarriers to subchannels is done using three major permutation methods called: partial usage of subchannels (PUSC), full usage of subchannels (FUSC) and adaptive modulation and coding (AMC). The subcarriers in a subchannel for first two methods are distributed throughout the available spectrum while these are contiguous in case of AMC. Resources of an OFDMA

system occupy place both in time (OFDM symbols) and frequency (subchannels) domains thus introducing both the time and frequency multiple access (Kulkarni et al., 2005).

Adaptive beamforming technique is a key feature of mobile WiMAX. It does not only enhance the desired directional signal but also its narrow beamwidth may reduce interference caused to the users in the neighboring cells. Resultant increase in signal to interference-plus-noise ratio (SINR) offers higher capacity and lower outage probability, which is defined as the probability that a user does not achieve minimum SINR level required to connect to a service. Adaptive beamforming can be used with PUSC, FUSC and AMC (refer Tab. 278 of IEEE standard 802.16-2005).

Network bandwidth is of high value for mobile network operators. It is always desired to get the maximum out of an available bandwidth by implementing frequency reuse 1 (network bandwidth being re-utilized in every sector see Fig. 1). However, with increased frequency reuse, radio quality of the users starts to deteriorate. Hence outage probability becomes more significant. To combat this problem, the conventional solution, in existing literature, is partial resource utilization or base station coordination to achieve frequency reuse 1.

Authors of (Porter et al., 2007) study the power gain, because of adaptive beamforming, of a IEEE 802.16e based system. Results presented by authors are based on measurements carried out in one sector of a cell with no consideration of interference. Measurements are carried out using an experimental adaptive beamforming system. Reference (Pabst et al., 2007) discusses the performance of WiMAX network using beamforming in conjunction with space division multiple access (SDMA). The simulations are carried out for OFDM (not OFDMA). Hence frequency diversity, because of distributed subcarrier permutations, is not taken into account. In (Necker, 2006) and (Necker, M. C., 2007), author has analyzed the performance of beamforming capable IEEE 802.16e systems with AMC. Unlike distributed subcarrier permutations (PUSC and FUSC), subcarriers in an AMC subchannel are contiguous on frequency scale. Hence PUSC/FUSC offer more frequency diversity as compared to AMC. Suggested interference coordination technique allows reuse 1 at the cost of reduced resource utilization. In (Maqbool et al., 2008a), we have carried out system level simulations for WiMAX networks. The analysis was focused on comparison of different frequency reuse patterns. Adaptive beamforming gain was also considered. We have shown that reuse 1 is possible with partial loading of subchannels.

In (Maqbool et al., 2008b), however, we have shown that by employing beamforming per PUSC group, the antenna-plus-array gain can be diversified and as a result reuse 1 is possible

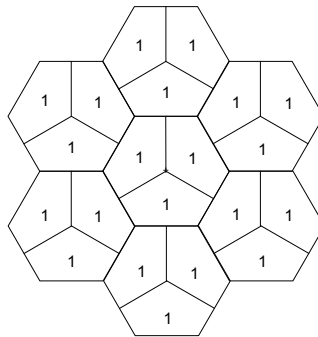


Fig. 1. Frequency Reuse Pattern 1x3x1.

without even partial loading of subchannels or base station coordination. In this chapter, we present results from (Maqbool et al., 2008b). We also extend those results by giving a comparison of system performance with all three subcarrier permutation types (PUSC, FUSC and AMC). The performance is analyzed in terms of cell throughput,  $SINR_{eff}$  and probability of outage. Monte Carlo simulations are carried out in downlink (DL) for this purpose.

Rest of the chapter is organized as follows: section 2 gives an introductory account of subcarrier permutation types to be analyzed in this chapter. Possibility of beamforming with different subcarrier permutation types is discussed in section 3. SINR, beamforming, physical abstraction model MIC, modulation and coding scheme (MCS) and simulator details are introduced in section 4. Simulation results have been presented in section 5. Finally section 6 discusses the conclusion of this analysis.

## 2. Subcarrier Permutation Types

In this section, we present the salient features of subcarrier permutation with PUSC, FUSC and AMC in DL. In Tab. 1, values of various parameters for each permutation scheme are listed. These values correspond to 10 MHz bandwidth.

A detailed account can be found in Maqbool et al. (2008c) where permutation method has been explained with the help of examples.

### 2.1 Partial Usage of Subchannels (PUSC)

One slot of PUSC DL is two OFDM symbols by one subchannel while one PUSC DL subchannel comprises of 24 data subcarriers. Subchannels are built as follows:

1. The used subcarriers (data and pilots) are sequentially divided among a number of physical clusters such that each cluster carries twelve data and two pilot subcarriers.
2. These physical clusters are permuted to form logical clusters using the renumbering formula on p. 530 in IEEE standard 802.16-2005. This process is called outer permutation. This permutation is characterized by a pseudo-random sequence and an offset called  $DL\_PermBase$ .
3. Logical clusters are combined together in six groups called the Major Groups. The even groups possess more logical clusters as compared to odd Major Groups. Throughout this chapter, we shall refer these Major Groups as groups only.
4. The assignment of subcarriers to subchannels in a group is obtained by applying Eq. 111 of IEEE standard 802.16-2005. This process is known as inner permutation. The assignment in inner permutation is also controlled by  $DL\_PermBase$ . Pilot subcarriers are specific to each group. Since number of logical clusters is different in even and odd groups, the number of their respective subchannels is also different.

### 2.2 Full Usage of Subchannels (FUSC)

The slot in FUSC mode is one OFDM symbol by one subchannel. Since slot in each permutation mode has same number of subcarriers, unlike in PUSC, the subchannel in FUSC comprises of 48 data subcarriers. Subcarriers are assigned to subchannels in the following manner:

1. Before subcarriers are assigned to subchannels, pilot subcarriers are first identified (subcarrier positions for pilot subcarriers are given in section 8.4.6.1.2.2 of IEEE standard 802.16-2005) and are separated from others. These pilot subcarriers are common to all subchannels.

Subcarrier Permutation	Parameter	Value
PUSC	No. of subchannels $N_{Sch}$	30
	No. of subchannels per even group $N_e$	6
	No. of subchannels per odd group $N_o$	4
	No. of PUSC groups	6
	No. of total data subcarriers	720
	No. of total pilot subcarriers	120
	No. of available slots in DL (considering 30 OFDM symbols in DL)	450
FUSC	No. of subchannels $N_{Sch}$	16
	No. of total data subcarriers	768
	No. of total pilot subcarriers	82
	No. of available slots in DL (considering 30 OFDM symbols in DL)	480
AMC	No. of subchannels $N_{Sch}$	48
	No. of total data subcarriers	768
	No. of total pilot subcarriers	96
	No. of available slots in DL (considering 30 OFDM symbols in DL)	480

Table 1. PUSC/FUSC/AMC parameters for 1024 FFT IEEE standard 802.16-2005.

2. In next step, the remaining subcarriers are divided among 48 groups.
3. Using Eq. 111 of IEEE standard 802.16-2005, a particular subcarrier is picked up from each group and is assigned to a subchannel. Similar to inner permutation of PUSC, this assignment is also controlled by  $DL\_PermBase$ .

In PUSC and FUSC, by using different  $DL\_PermBase$  in network cells, subcarriers of a given subchannel are not identical in adjacent cells. In this case, it has been shown in (Ramadas & Jain, 2007) and (Lengoumbi et al., 2007), that the above process is equivalent to choosing subcarriers using uniform random distribution on the entire bandwidth in every cell. During our simulations, we consider the same assumption.

### 2.3 Adaptive Modulation and Coding (AMC)

In adjacent subcarrier permutation mode AMC, a slot is defined as  $N_b$  bins  $\times$   $M$  OFDM symbols, where ( $N_b \times M = 6$ ). All available subcarriers (data+pilot) are sequentially grouped into bins. A bin is composed of nine contiguous subcarriers such that eight are data and one is pilot subcarrier. Though not exclusively specified in IEEE standards 802.16-2004 and 802.16-2005, but in consistent with nomenclature of PUSC and FUSC, we call ensemble the bins in a slot as subchannel. Out of possible combinations, we choose 2 bins  $\times$  3 OFDM symbols in our simulations.

## 3. Subcarrier Permutation and Beamforming

Pilot subcarriers are required for channel estimation. In case of beamforming, dedicated pilots are required for each beam in the cell. For PUSC and FUSC, there is a common set of pilot sub-

carriers for a number of subchannels while in AMC mode, each subchannel has its own pilot subcarriers. Hence, the number of possible orthogonal beams in a cell (of cellular network) depends upon the distribution of pilot subcarriers and hence the subcarrier permutation type. In PUSC, subchannels are put together in six groups. Each group has its own set of pilot subcarriers and hence, beamforming can be done per PUSC group. As subcarriers of a subchannel are chosen randomly, each subcarrier may experience the interference from different beams of a given interfering cell. In this way, subcarriers of a subchannel will not experience the same interference. The value of interference will depend upon array-plus-antenna gain of the colliding subcarrier that may belong to any of six interfering beams in neighboring cell.

Pilot subcarriers in FUSC are common to all subchannels. Hence a single beam is possible in every cell. In contrast to PUSC, all subcarriers of a subchannel experience the same interference. This is due to the fact that every colliding subcarrier will have the same array-plus-antenna gain since there is only one beam per interfering cell.

When we consider AMC for beamforming, there can be as many orthogonal beams as the number of subchannels since every subchannel has its own pilot subcarriers. Due to similar assignment of subcarriers to subchannels in neighboring cells, all subcarriers will experience the same amount of interference because of an interfering beam in the neighbouring cell. Colliding subcarriers in a beam will have same array-plus-antenna. In addition, unlike PUSC and FUSC, since subcarriers of a subchannel are contiguous in AMC, no diversity gain is achieved.

## 4. Network and Interference Model

### 4.1 Subcarrier SINR

SINR of a subcarrier  $n$  is computed by the following formula:

$$SINR_n = \frac{P_{n,Tx} a_{n,Sh}^{(0)} a_{n,FF}^{(0)} \frac{K}{d^{(0)\alpha}}}{N_0 W_{Sc} + \sum_{b=1}^B P_{n,Tx} a_{n,Sh}^{(b)} a_{n,FF}^{(b)} \frac{K}{d^{(b)\alpha}} \delta_n^{(b)}} \quad (1)$$

where  $P_{n,Tx}$  is the per subcarrier power,  $a_{n,Sh}^{(0)}$  and  $a_{n,FF}^{(0)}$  represent the shadowing (log-normal) and fast fading (Rician) factors for the signal received from serving BS respectively,  $B$  is the number of interfering BS,  $K$  is the path loss constant,  $\alpha$  is the path loss exponent and  $d^{(0)}$  is the distance between MS and serving BS. The terms with superscript  $b$  are related to interfering BS.  $W_{Sc}$  is the subcarrier frequency spacing,  $N_0$  is the thermal noise density and  $\delta_n^{(b)}$  is equal to 1 if interfering BS transmits on  $n^{th}$  subcarrier and 0 otherwise.

### 4.2 Effective SINR

Slot is the basic resource unit in an IEEE 802.16 based system. We compute  $SINR_{eff}$  over the subcarriers of a slot. The physical abstraction model used for this purpose is MIC (Ramadas & Jain, 2007) and is explained hereafter.

After calculating SINR of  $n^{th}$  subcarrier, its spectral efficiency is computed using Shannon's formula:

$$C_n = \log_2 (1 + SINR_n) [bps/Hz],$$

MIC is computed by averaging spectral efficiencies of  $N'$  subcarriers of a slot:

$$MIC = \frac{1}{N'} \sum_{n=1}^{N'} C_n [bps/Hz],$$

at the end  $SINR_{eff}$  is obtained from MIC value using following equation:

$$SINR_{eff} = 2^{MIC} - 1.$$

For computation of  $SINR_{eff}$ , log-normal shadowing is drawn randomly for a slot and is same for all subcarriers of a slot. In presence of beamforming, it is essential to know the exact location of MS in the cell. For that purpose, line of sight (LOS) environment has been considered in simulations. Hence for fast fading, Rice distribution has been considered. Rician K-factor has been referred from (D.S. Baum et al., 2005) (scenario C1). Since in PUSC and FUSC, subcarriers of a subchannel (hence a slot) are not contiguous, fast fading is drawn independently for every subcarrier of a slot (Fig.2). On the other hand, the subcarriers in an AMC slot are contiguous and hence their fast fading factor can no longer be considered independent and a correlation factor of 0.5 has been considered in simulations. Coherence bandwidth is calculated by taking into account the powers and delays of six paths of vehicular-A profile with speed of MS equal to 60 Km/h (Tab. A.1.1 of (Ramadas & Jain, 2007)) and is found to be 1.12 MHz.

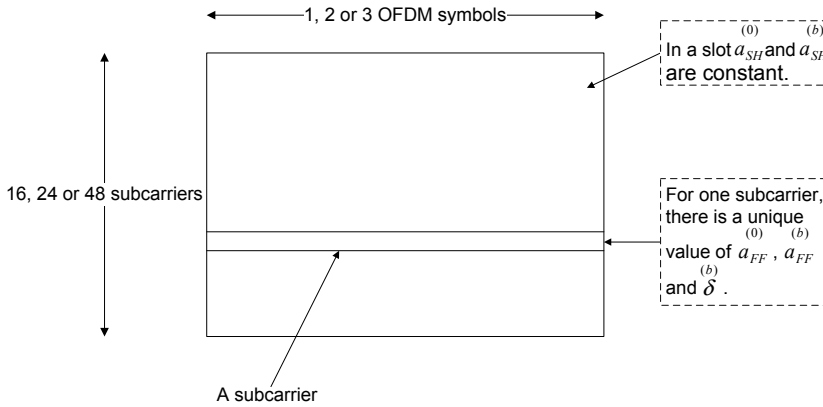


Fig. 2. Shadowing and fast fading over a PUSC/FUSC/AMC slot.

### 4.3 Beamforming Model

The beamforming model considered in our simulation is the delay and sum beamformer (or conventional beamformer) with uniform linear array (ULA). The power radiation pattern for a conventional beamformer is a product of array factor and radiation pattern of a single antenna. The array factor for this power radiation pattern is given as (Tse & Viswanath, 2006):

$$AF(\theta) = \frac{1}{n_t} \left| \frac{\sin\left(\frac{n_t \pi}{2} (\cos(\theta) - \cos(\phi))\right)}{\sin\left(\frac{\pi}{2} (\cos(\theta) - \cos(\phi))\right)} \right|^2, \quad (2)$$

where  $n_t$  is the number of transmit antennas at BS (with inter-antenna spacing equal to half wavelength),  $\phi$  is the look direction (towards which the beam is steered) and  $\theta$  is any arbitrary direction. Both these angles are measured with respect to array axis at BS (see Fig.3).

The gain of single antenna associated with array factor is given by Eq.3 (Ramadas & Jain, 2007):

$$G(\psi) = G_{max} + \max \left[ -12 \left( \frac{\psi}{\psi_{3dB}} \right)^2, -G_{FB} \right], \quad (3)$$

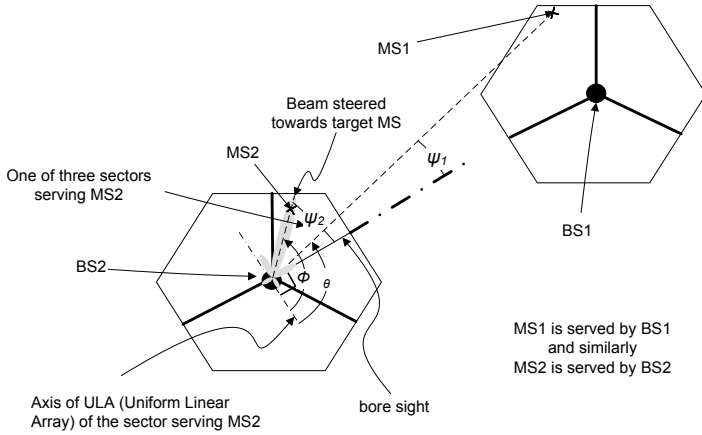


Fig. 3. Example showing beamforming scenario.

where  $G_{max}$  is the maximum antenna gain in boresight direction,  $\psi$  is the angle MS subtends with sector boresight such that  $|\psi| \leq 180^\circ$ ,  $\psi_{3dB}$  is the angle associated with half power beamwidth and  $G_{FB}$  is the front-to-back power ratio.

#### 4.4 Path Loss Model

Line-of-sight (LOS) path loss (PL) model for suburban macro (scenario C1) has been referred from D.S. Baum et al. (2005). It is a three slope model described by the following expressions:

$$PL(d) = \begin{cases} \text{free space model} & \text{if } d \leq 20m; \\ C(f_c) + 23.8 \log_{10}(d) & \text{if } 20m < d \leq d_{BP}; \\ C(f_c) + 40 \log_{10}(d/d_{BP}) + 23.8 \log_{10}(d_{BP}) & \text{if } d > d_{BP}, \end{cases}$$

where  $f_c$  is the carrier frequency in Hz,  $C(f_c)$  is the frequency factor given as:  $33.2 + 20 \log_{10}(f_c/2 \cdot 10^9)$ ,  $d_{BP}$  is the breakpoint distance and  $\sigma_{Sh}$  is the standard deviation of log-normal shadowing. The breakpoint distance is computed as:  $d_{BP} = 4h_{BS}h_{MS}/\lambda_c$ , with  $h_{BS}$  and  $h_{MS}$  being the heights of BS and MS respectively. The value of  $\sigma_{Sh}$  associated with above model is 4 dB for  $d \leq d_{BP}$  and is equal to 6 dB beyond  $d_{BP}$ .

#### 4.5 Modulation and Coding Scheme (MCS)

One of the important features of IEEE 802.16 based network is assignment of MCS type to a user depending upon its channel conditions. We have considered six different MCS types in our simulation model: QPSK-1/2 (the most robust), QPSK-3/4, 16QAM-1/2, 64QAM-2/3 and 64QAM-3/4 (for the best radio conditions). SINR threshold values for MCS types are given in Tab.2 and have been referred from *WiMAX Forum Mobile System Profile* (2007). If SINR of a mobile station (MS) is less than the threshold of the most robust MCS (i.e., less than 2.9 dB), it can neither receive nor transmit anything and is said to be in outage.



Index	1	2	3	4	5	6
MCS	QPSK 1/2	QPSK 3/4	16QAM 1/2	16QAM 3/4	64QAM 2/3	64QAM 3/4
$SINR_{eff}$ [dB]	2.9	6.3	8.6	12.7	16.9	18

Table 2. Threshold of  $SINR_{eff}$  values for six MCS types *WiMAX Forum Mobile System Profile* (2007).

#### 4.6 Simulator Details

The frequency reuse pattern considered in simulations is 1x3x1 (Fig.1). The number of cells in the network is nineteen (i.e., eighteen interfering BS). To speed up the simulation process and to include the effect of an infinite network, wraparound technique has been employed. A significant number of snapshots are being carried out for Monte Carlo simulations. Locations of MS in a sector are drawn using uniform random distribution and beams are steered according to these locations. At BS, four transmitting antennas have been considered while MS is supposed to possess one receiving antenna. All simulations are carried out with full loading of subchannels.

As explained earlier, when PUSC is used, there can be up to six beams per sector i.e., one beam per group. For simulations with PUSC, we have considered three different cases with 1, 3 and 6 adaptive beams respectively. For the first case, all six PUSC groups are used by one beam. In the second case, each beam uses one odd and one even group. In the last case, each beam uses a distinct group. It is to be noted that number of channels per even and odd group are different (see Tab.1). To find the direction of adaptive beams, equivalent number of MS are drawn in a cell using spatial uniform distribution.

For the first case, one MS is drawn per sector and all subcarriers of a slot experience the same interfering beam pattern from a neighboring sector. On the other hand, in the second case, three MS are dropped in a sector and hence there are three interfering beams per sector. For each subcarrier used by a MS, the interfering beam is chosen with equal probability.

When there are six beams in a sector, the selection of interfering beam per subcarrier is no more equally probable. The reason being that beams are associated to even or odd groups and thus have different number of subchannels. Hence, for a subcarrier, the probability of interfering with an even beam is given as:

$$p_e = \frac{N_e}{N_{Sch}},$$

and with an odd beam it is:

$$p_o = \frac{N_o}{N_{Sch}}.$$

Considering a subcarrier, six MS are drawn per interfering sector. Respective beams are steered, three of them are odd and the others three are even. In a given interfering sector, the chosen beam is drawn according to the above discrete distribution.

In case of FUSC and AMC, one MS is drawn per sector and all subcarriers of a slot experience the same interfering beam pattern from a neighboring sector.

During every snapshot,  $SINR_{eff}$  of a MS is calculated using MIC model. Cell space around BS is divided into twenty rings. Since MS is dropped using uniform random distribution,

Parameter	Value
Carrier frequency $f_c$	2.5 GHz
BS rms transmit power $P_{Tx}$	43 dBm
Subcarrier spacing $\Delta f$	10.9375 kHz
No. of DL OFDM Symbols $N_S$	30
Thermal noise density $N_0$	-174 dBm/Hz
One side of hexagonal cell $R$	1.5 Km
Height of BS $h_{BS}$	32 m
Height of MS $h_{MS}$	1.5 m
Antenna Gain (boresight) $G_{max}$	16 dBi
Front-to-back power ratio $G_{FB}$	25 dB
3-dB beamwidth $\psi_{3dB}$	70°
No. of transmitting antennas per sector for beamforming $n_t$	4

Table 3. Parameters of simulations (Ramadas &amp; Jain, 2007).

during a snapshot, it might be located in any of the twenty rings.  $SINR_{eff}$  and throughput are averaged over each of these rings and over complete cell as well. The former is used to study the effect of change in the values of  $SINR_{eff}$  and throughput w.r.t. distance from the BS. If  $SINR_{eff}$  value of a MS during a snapshot is less than 2.9 dB (threshold value being referred from *WiMAX Forum Mobile System Profile* (2007)), it is considered to be in outage. Throughput of a MS during a snapshot, depends upon the MCS used by it. Simulation parameters are given in Tab.3. The parameter values are mainly based on (Ramadas & Jain, 2007).

## 5. Simulation Results

In this section we present the simulation results. Since PUSC has three possibilities for implementation of beamforming (cf. section 4.6), we first present results for three possible cases of PUSC. We compare these results with a case when beamforming is not considered. We call it without beamforming case. In addition, a scenario assuming beamforming only in the serving cell is also presented. Average  $SINR_{eff}$  and average global throughput with respect to distance from BS are presented in Fig.4 and 5 respectively.

A clear difference can be observed between beamforming and without beamforming cases. We can observe about 7 to 8 dB gain. The gain for "beamforming in the serving cell only" scenario is about 2 dB less. The difference shows the effect of beamforming on interference reduction. The difference in terms of  $SINR_{eff}$  and global throughput is not much with varying number of interfering beams.

However, it can be clearly seen in Fig.6 that outage probability significantly decreases when we take full advantage of diversity offered by PUSC. When increasing the number of beams, outage probability decreases from an unacceptable 9% (with one beam) to a reasonable 2% (with six beams). It is interesting to note that average throughput and  $SINR_{eff}$  are not affected by the gain in outage probability. It can also be noticed that outage probability of "beamforming in the serving cell only" scenario is quite small. The reason being, the signal

strength in the serving cell is increased because of beamforming while absence of beamforming in interfering cells keeps the interference strength unchanged.

Next we compare the results of three subcarrier permutation types. In this comparison, PUSC has been considered with six interfering beams. In Fig. 7, average values of effective SINR ( $SINR_{eff}$ ) are plotted as a function of distance from base station (BS). As can be noticed, there is almost no difference between values of  $SINR_{eff}$  with PUSC, FUSC and AMC. On the other hand, when we look at MCS probabilities in Fig. 9, PUSC outclasses the other two (FUSC and AMC) in terms of outage probabilities. Though average  $SINR_{eff}$  are same for all, only PUSC offers an outage probability in an acceptable range (less than 5%). Since subcarriers in a PUSC subchannel experience variable interference gains, it average outs the possibility of all subcarriers suffering from same and high interference. That is why outage probability is reduced. At the same time, it also reduces the probability that all colliding subcarriers have low power. This effect can be noticed while looking at probabilities of high rate MCS. For example, with PUSC, probability to transmit with 64QAM-3/4 is less as compared to FUSC and AMC.

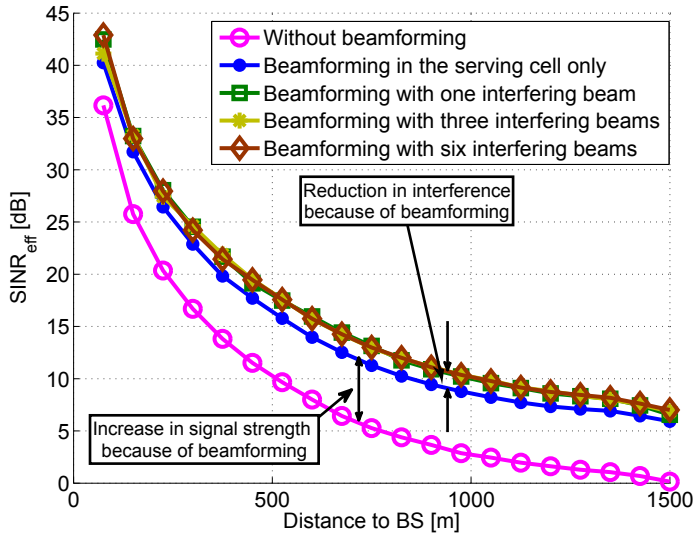


Fig. 4. Average  $SINR_{eff}$  versus distance to base station for PUSC.

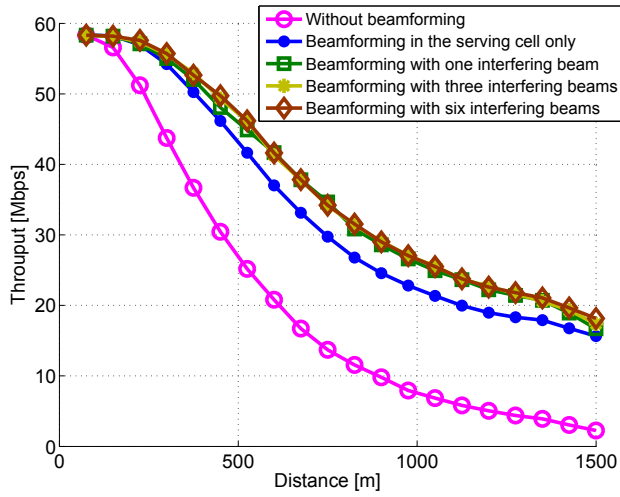


Fig. 5. Average cell throughput versus distance to base station for PUSC.

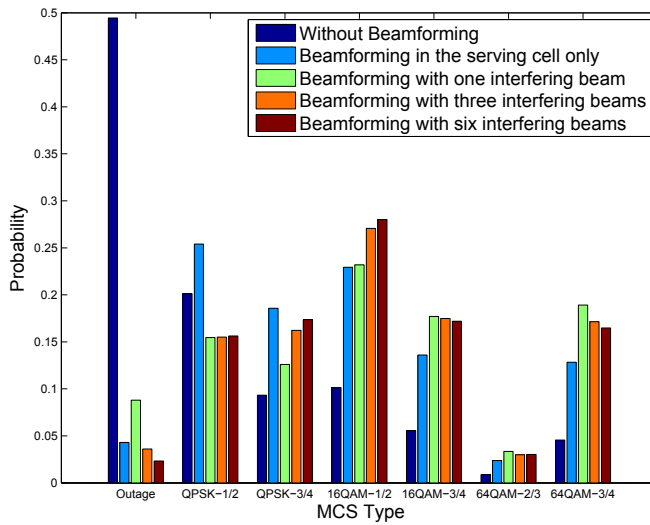


Fig. 6. MCS distribution for PUSC.

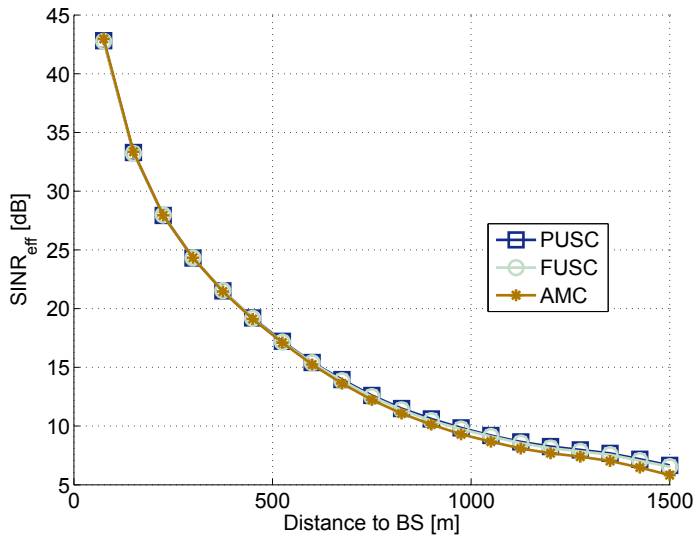


Fig. 7. Average  $SINR_{eff}$  versus distance to base station for PUSC/FUSC/AMC with beamforming.

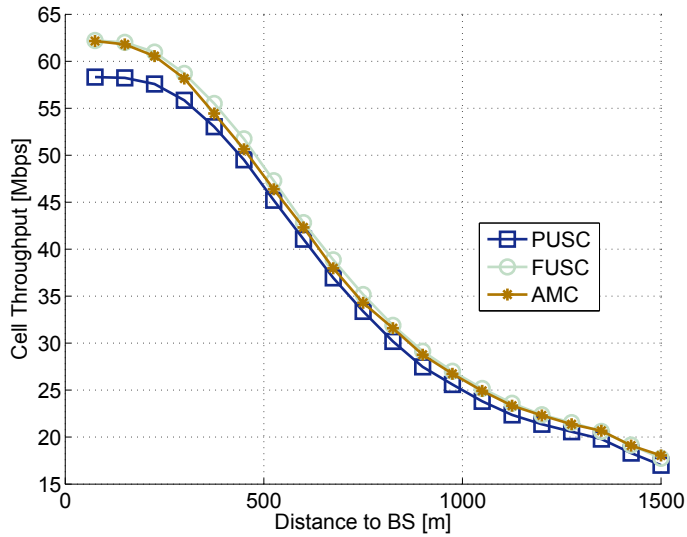


Fig. 8. Average cell throughput versus distance to base station for PUSC/FUSC/AMC with beamforming.

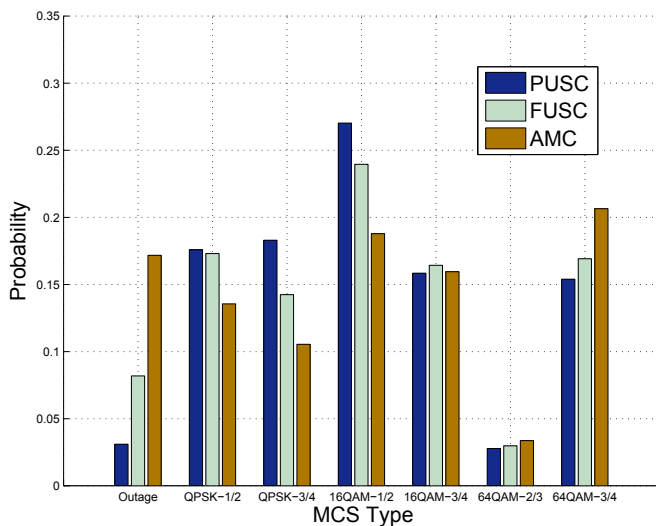


Fig. 9. MCS distribution for PUSC/FUSC/AMC with beamforming.

If we look at average values of cell throughput (w.r.t. distance from BS) in Fig. 8, it can be noticed that in the region close to BS, PUSC is somewhat less performing than FUSC and AMC. This result can be justified in light of probabilities of MCS in Fig. 9 where stationary probabilities of the best MCS (64QAM-3/4) are higher with FUSC and AMC. Owing to strong signal strength in the region close to base station, probability for a MS to achieve better MCS is more. At about 350 m and onward (from base station), throughput with PUSC is around 1 Mbps less than that of FUSC and AMC even if PUSC has better performance in terms of radio quality. This is because of the fact that with PUSC, number of available slots are lesser (see Tab. 1).

## 6. Conclusion

Currently, WiMAX networks are going through trial and deployment phase. Therefore, it is important at this stage to analyze various features of WiMAX. In this chapter, we have studied the possibility of adaptive beamforming in connection with three subcarrier permutation types of WiMAX. We have shown that beamforming per PUSC group offers a low outage probability as compared to FUSC and AMC. FUSC and AMC have more number of data subcarriers and hence the resultant throughput with the two is slightly more than that of PUSC. At the same time, outage probabilities for FUSC and AMC are more than 5%. Hence, adaptive beamforming per PUSC group can be exploited to achieve acceptable radio quality without need of partial loading of subchannels or base station coordination.

## 7. References

D.S. Baum et al. (2005). IST-2003-507581, D5.4 Final Report on Link and System Level Channel Models. WINNER.

URL: <https://www.ist-winner.org/DeliverableDocuments/D5.4.pdf>

- Kulkarni, G., Adlakha, S. & Srivastava, M. (2005). Subcarrier Allocation and Bit Loading Algorithms for OFDMA-Based Wireless Networks, *IEEE Trans. on Mobile Computing*, Vol. 4.
- Lengoumbi, C., Godlewski, P. & Martins, P. (2007). Subchannelization Performance for the Downlink of a Multi-Cell OFDMA System, *Proc. of IEEE WiMob*.
- Maqbool, M., Coupechoux, M. & Godlewski, P. (2008a). Comparison of Various Frequency Reuse Patterns for WiMAX Networks with Adaptive Beamforming, *Proc. of IEEE VTC Spring*.
- Maqbool, M., Coupechoux, M. & Godlewski, P. (2008b). Effect of Distributed Subcarrier Permutation on Adaptive Beamforming in WiMAX Networks, *Proc. of IEEE VTC Fall*.
- Maqbool, M., Coupechoux, M. & Godlewski, P. (2008c). Subcarrier Permutation Types in IEEE 802.16e, *Technical report*, TELECOM ParisTech.
- Necker, M. C. (2006). Towards Frequency Reuse 1 Cellular FDM/TDM Systems, *ACM MSWiM*.
- Necker, M. C. (2007). Coordinated Fractional Frequency Reuse, *ACM MSWiM*.
- Pabst, R., Ellenbeck, J., Schinnenburg, M. & Hoymann, C. (2007). System Level Performance of Cellular WiMAX IEEE 802.16 with SDMA-enhanced Medium Access, *Proc. of IEEE WCNC*, pp. 1820–1825.
- Porter, J. W., Kepler, J. F., Krauss, T. P., Vook, F. W., Blankenship, T. K., Desai, V., Schooler, A. & Thomas, J. (2007). An Experimental Adaptive Beamforming System for the IEEE 802.16e-2005 OFDMA Downlink, *Proc. of IEEE Radio and Wireless Symposium*.
- Ramadas, K. & Jain, R. (2007). WiMAX System Evaluation Methodology, *Technical report*, Wimax Forum.
- Tse, D. & Viswanath, P. (2006). *Fundamentals of Wireless Communications*, Cambridge University Press.
- WiMAX Forum Mobile System Profile (2007).